



ELSEVIER

Journal of Chromatography A, 853 (1999) 309–319

JOURNAL OF
CHROMATOGRAPHY A

Detection of duck hepatitis B virus DNA fragments using on-column intercalating dye labeling with capillary electrophoresis–laser-induced fluorescence

W.G. Tan^a, D.L.J. Tyrrell^a, N.J. Dovichi^{b,*}

^aGlaxo Heritage Research Institute, Department of Medical Microbiology and Immunology, University of Alberta, Edmonton, Alberta, T6G 2H7 Canada

^bDepartment of Chemistry, University of Alberta, Edmonton, Alberta, T6G 2G2 Canada

Abstract

A rapid on-column DNA labeling technique is used to detect viral restriction DNA fragments by capillary electrophoresis–laser induced fluorescence detection. Intercalating dyes such as POPO3 or ethidium homodimer-2 are incorporated into the detection buffer. The cationic dyes migrate into the capillary during electrophoresis and bind to the oppositely migrating DNA fragments. A post-column sheath-flow fluorescence detector is used in the experiment. Excellent labeling efficiency is achieved at minimal background fluorescence by diluting the dyes to between $1 \cdot 10^{-7} M$ and $5 \cdot 10^{-7} M$ in a buffer with low ionic strength relative to the running buffer within the capillary. This dilute sheath-flow buffer allows stacking of dye molecules inside the capillary when an electric field is applied. Calibration curves using a series of DNA size markers (between 72 and 1353 base pairs) were linear over an order of magnitude in DNA concentration. Sensitivity also increased linearly with fragment length, and detection limits ranged from $4 \cdot 10^{-14} M$ to $5 \cdot 10^{-13} M$ for the size-standards. Analysis of cloned viral DNA using duck hepatitis B virus demonstrated a concentration detection limit of $3.9 \cdot 10^{-16} M$. Last, the technique produced very high separation efficiency, $14 \cdot 10^6$ theoretical plates which is greater than $47 \cdot 10^6$ plates m^{-1} , for the duck hepatitis B viral genome. © 1999 Elsevier Science B.V. All rights reserved.

Keywords: Hepatitis B virus; DNA; Dyes

1. Introduction

Hepatitis B virus (HBV) DNA is the most reliable marker for monitoring HBV infections because HBV enters the blood when there is active viral replication in the liver [1]. We are interested in detecting HBV sequence in human sera without sequence amplification using polymerase chain reaction (PCR). Rather than working with the highly infectious human virus,

we work with a related virus, duck hepatitis B virus (DHBV), which infects an animal model. In this study, we employed capillary electrophoresis to assay restriction digests of cloned DHBV genome. The use of capillary electrophoresis for analysis of double stranded DNA has a rich history, including the analysis of restriction DNA fragments [2–8], detection of point mutation in DNA and PCR products [5,7,9–11].

Analysis of DNA fragments using intercalating dyes has been studied extensively [2,12–19]. The binding of these dyes usually follows the “neigh-

*Corresponding author.

boring exclusion principle” where every second site along the double helix remains unoccupied [20]. Many of these cationic dyes, in particular the dimeric analogs of acridines [21–23], demonstrate DNA-binding affinities several orders of magnitude higher than their corresponding monomers. Using a pre-column staining method, Zhu described the use of thiazole orange homodimer TOTO to detect DNA fragment as dilute as $40 \text{ fg } \mu\text{l}^{-1}$ [16]. Figeys showed detection limits of a few octomoles of fluorescently labeled DNA using dimeric dyes POPO3, YOYO3 and YOYO1 in high salt buffer [14]. Skeidsvoll demonstrated the use of SYBR Green I, a monomeric fluorescent dye, for the detection of DNA fragments separated in hydroxypropyl methylcellulose [24].

Complicated band splitting pattern or band-broadening have been reported in cases where DNA fragments were pre-stained prior to sample loading and DNA separation was carried out without incorporating intercalating dyes into the electrophoresis buffer [16,19,25,26]. This phenomenon can be reasoned by the equilibrium between the dye and the DNA molecules. When the DNA–dye complexes migrate toward the detection end, they traverse in a dye-depleted zone as the unbound dye molecules migrate toward the injection end. The complexation equilibrium will favor the formation of free dye and DNA in this dye-depleted region. The loss of dye results in a heterogeneous distribution in the number of dye molecules complexed with the DNA strands, which leads to peak broadening.

Some groups have reported success with the use of dimeric dyes to generate DNA separations with efficiency no different from that with monomeric dyes [14,24,27]. This observation reflects the technical variation in separation parameters such as DNA–dye incubation period, the incorporation of dyes into the sieving matrix and the presence or absence of excess dye in the electrophoresis and separation buffers. In the case where NaCl is added to the separation buffer, separation of POPO3-labeled fragments resulted in separation efficiencies in excess of $2 \cdot 10^6$ plates for small DNA fragments [14]. The addition of NaCl in the separation buffer increases the thermal stability of the DNA double helix, which stabilizes the DNA–dye complexes during electrophoresis. When fluorescent dye was added to both

the electrophoresis and separation buffers, DNA peaks were symmetrical, and the separation efficiency for the large DNA fragments was on the order of $3 \cdot 10^6$ plates meter⁻¹ [27].

Most of the DNA–dye intercalation studies require DNA–dye incubation to allow the dye molecules homogeneously distribute themselves along the DNA. Using bis-intercalating dyes, Carlsson et al. [25] have demonstrated that this equilibration process is extremely slow at room temperature, but can be improved if the temperature of incubation is raised to 50°C, where the DNA–dye complexes equilibrate completely in 2 h.

We have employed an on-column labeling method that allows simultaneous labeling and separation of DNA restriction fragments without the need for a pre-staining step. DNA separation is carried out in a discontinuous electrolyte system where buffer at the detection end is doped with intercalating dyes. This buffer carries an ionic strength half of that present in the sieving matrix and the separation buffer to allow stacking of dye molecules in the capillary during electrophoresis. Detection of DNA fragments is achieved in a post-column configuration using a sheath flow cuvette system [28]. Application of high electric field strength separation is demonstrated using dimeric intercalating dyes. Separation of DNA fragments from various molecular size markers are used to define DNA concentration linearity, dynamic range and detection limit. These parameters are used in turn to characterize the cloned DHBV genome.

2. Experimental

2.1. Apparatus

The instrument for capillary electrophoresis was built locally and has been described in detail elsewhere [28]. Separation was driven with a high-voltage power supply (Model CZE 1000R, Spellman High Voltage Electronics, Plainview, NY, USA). The injector was equipped with a locally constructed Plexiglas box with safety interlock. Fluorescence was excited in a sheath flow cuvette (1 mm thick walls, $200 \mu\text{m} \times 200 \mu\text{m}$ square inner bore). Fluorescence was excited with a 543.5 nm He–Ne laser (1 mW output, Melles Griot) and detected with an

R1477 photomultiplier tube (Bridgewater, NJ, USA). An interface box (I-V converter) transferred output from the instrument to the computer. A Macintosh Centris 650 computer controlled the power supply and monitored the fluorescence signal at 10 Hz via a NB-MIO-16XH-18 input/output board (National Instruments, Austin, TX, USA).

2.2. Parameters of CE separation

Separation was performed using a 30 cm×50 μm I.D.×144 μm O.D. DB-210 coated fused-silica capillary purchased from J&W Scientific (Folsom, CA, USA). Electrophoresis buffer was TBE containing 90 mM Tris–borate and 2 mM EDTA at pH 8.6. Unless otherwise indicated, the detection end of the capillary was installed inside the sheath flow cuvette containing intercalating dye in 45 mM Tris base and 1 mM EDTA buffer at pH 7. Sample introduction was performed by electrokinetic injection at 1 kV for 5 to 10 s, and separation was performed with an electric field of 200 V/cm or

higher. A 0.8% (w/v) hydroxyethylcellulose (HEC; M_r 250 000, Sigma) was prepared in electrophoresis buffer, filtered by Millex-GS 0.45 μm filter unit (Millipore, Bedford, MA, USA) and used as the sieving matrix.

2.3. Preparation of restriction DNA

Molecular size markers ΦX-174/*HaeIII* digest were purchased from Pharmacia Biotech (Piscataway, NJ, USA) and 1kilobase pair DNA size markers were purchased from Gibco BRL (Life Technologies). Dilution of DNA samples was carried out in deionized water unless otherwise indicated. All DNA samples were freshly prepared and stored on dry ice prior to sample injection.

2.4. Preparation of DHBV plasmid DNA

Plasmid pAltD2–8 was a gift from Dr. K. Fisher (Glaxo Heritage Research Institute). It contained a 3021 base pairs (bp) monomer of the duck hepatitis

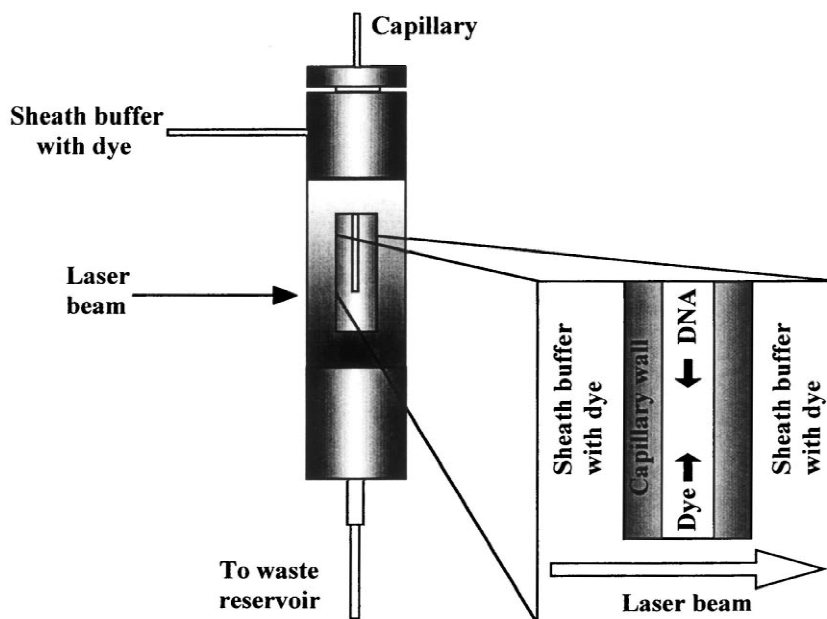


Fig. 1. Schematic diagram of a sheath flow cuvette. The sheath flow cuvette is connected to a buffer reservoir via teflon tubing. The buffer reservoir carried electrophoresis buffer containing intercalating dyes. The buffer is siphoned into the cuvette chamber where the detection end of the capillary is secured. When voltage is applied across the capillary, the positively charged dye molecules migrate into the capillary at its detection end, moving towards the injection end. A difference in buffer ionic strength between the sieving matrix in the capillary and the electrophoresis buffer creates a stacking effect at the end of the capillary, results in rapid migration of dye molecules into the capillary.

B virus (DHBV) genome cloned into the *EcoRI* site of vector pAlter-1 (Promega). The plasmid was propagated in *E. coli* strain DH 5 α grown in suspension broth culture. pAltD2–8 DNA was recovered using Qiagen Plasmid Purification Kit (Qiagen, Chatworth, CA, USA). The isolated plasmid was digested with restriction endonuclease *EcoRI* and then purified by QIAquick PCR purification (Qiagen). The concentration of the purified DNA was determined by optical absorbance at 260 nm. To remove the vector from the DHBV genome, plasmid digested with *EcoRI* was resolved by electrophoresis on a 0.8% agarose gel. The fragment corresponded to the 3021 bp monomer was excised and purified using QIAquick Gel Extraction Kit (Qiagen). Briefly, gel slices containing the 3021 bp monomer were dissolved in Qiagen QG buffer at

50°C before loading onto the QIAquick column. After one wash with 500 μ l QG buffer and two washes with 750 μ l PE buffer, the DNA was eluted with EB buffer.

3. Results and discussion

We wish to employ a rapid, sensitive, and efficient separation method for double stranded DNA. We chose to use on-column labeling of DNA to eliminate the tedious equilibrium step associated with pre-column staining of DNA with intercalating dyes. To prevent the depletion of the dye at the detection end of the capillary, we filled both the capillary and the detection buffer reservoir with the intercalating dye. The movement of dye molecules into the sheath

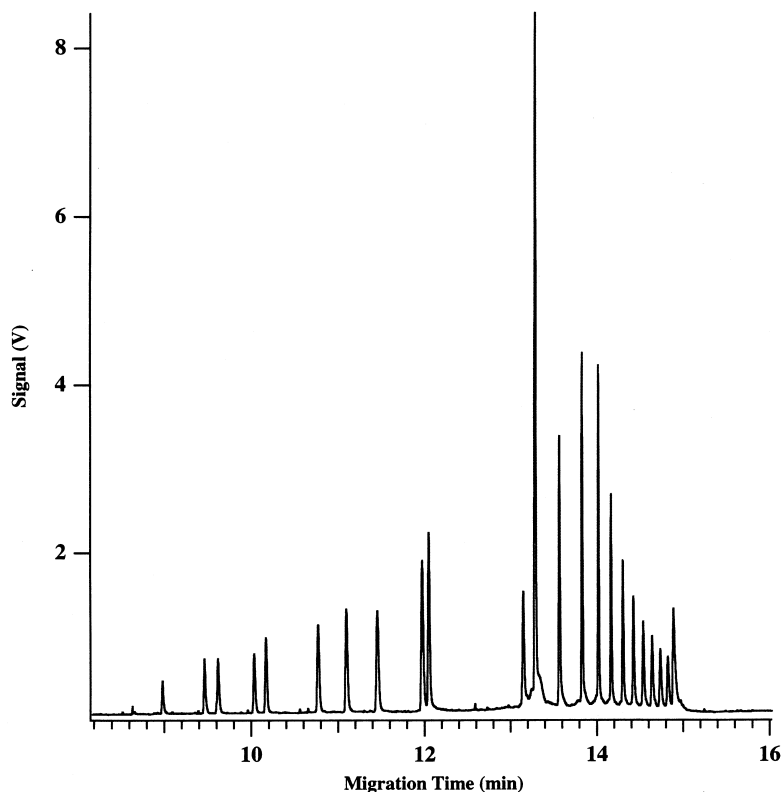


Fig. 2. Separation of 1 kb DNA ladder in 0.8% HEC. Stock DNA was diluted to 2.5 ng/ μ l in 9 mM Tris–borate and 200 μ M EDTA at pH 8.6. Sieving matrix was prepared using running buffer containing 90 mM Tri–borate and 2 mM EDTA (pH 8.6). POPO-3 was diluted to $2 \cdot 10^{-7}$ M in 45 mM Tris base and 1 mM EDTA (pH 7) and introduced into the sheath flow cuvette by siphoning. DNA was injected at 1000 V for 5 s and separated at 200 V/cm. Sizes in base pairs of the 23 DNA fragments (starting from the left) are: 72, 134, 154, 201, 220, 298, 344, 396, 506, 517, 1018, 1636, 2036, 3054, 4072, 5090, 6108, 7126, 8144, 9162, 10 180, 11 198, 12 216.

flow cuvette is depicted in Fig. 1. To reduce the contribution of this dye to the background fluorescence signal, we used a post-column fluorescence detector with a discontinuous buffer system. This detection-end discontinuous buffer system appears to be unique. It allowed the use of a relatively low concentration dye concentration in the detection region to reduce the background signal while producing a higher dye concentration in the separation capillary to efficiently label DNA fragments.

3.1. Separation efficiency

Fig. 2 shows the separation of 1 kb DNA ladder, with all 23 fragments resolved in a 0.8% HEC

matrix. In CE, using cellulose as the sieving medium, the larger fragments are often difficult to resolve [8,24]. The short contact time of the DNA with the dye during the separation does not degrade the separation resolution.

Extraordinarily high separation efficiency is produced for large DNA fragments in this separation medium. Fig. 3 presents the separation of a 3021 bp DHBV genome from a 5680 bp vector. The separation efficiency for the DHBV is $14 \cdot 10^6$ plates ($47 \cdot 10^6$ plates m^{-1}) in both electropherograms, correcting for peak asymmetry. The larger fragment generated a peak with significant tailing, and had only $3.8 \cdot 10^6$ plates ($13 \cdot 10^6$ plates m^{-1}). These are among the highest efficiency reported for any separation technique. These data were obtained with a

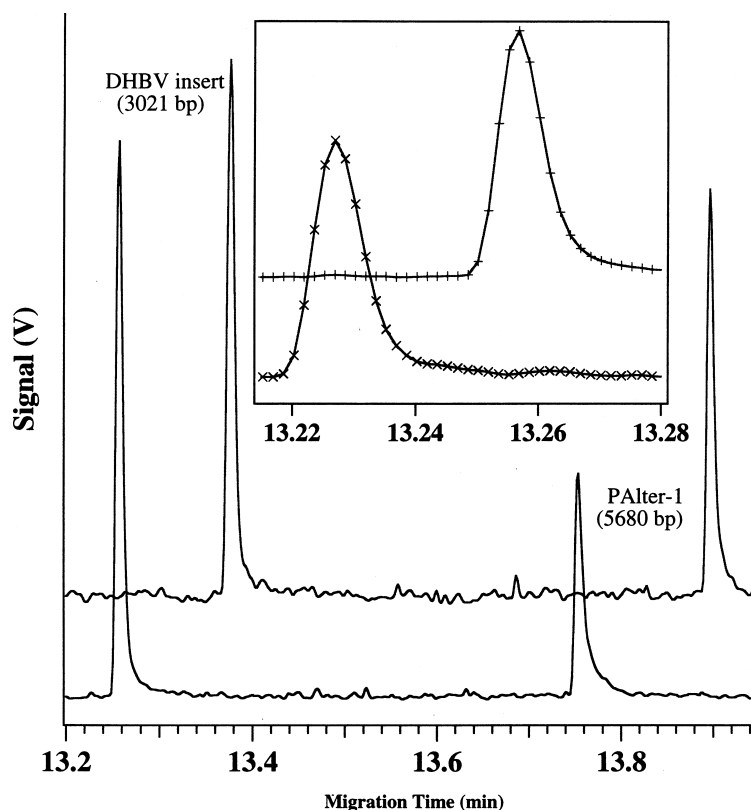


Fig. 3. High separation efficiency of large DNA fragments. The 3021 bp duck hepatitis B virus insert was removed from the vector (PAlter-1) by endonuclease *EcoRI* digestion at 37°C for 3 h. The electropherograms were obtained from two consecutive injections of the digested sample. The sieving matrix was the same as Fig. 2. POPO-3 was diluted to $2 \cdot 10^{-7}$ M in 45 mM Tris base and 1 mM EDTA (pH 10.4) and introduced into the sheath flow cuvette by siphoning. The shorter fragment is the 3021 bp insert and the larger fragment is the 5680 bp vector. The insert shows an expanded view of the peak generated by the 3021 bp fragment. Injection was at 1000 V for 5 s.

sheath-flow buffer that had been adjusted to pH 10.4 to improve the sensitivity of the measurement. Similar plate counts were observed with a sheath-flow buffer at pH 7.9.

3.2. Stacking of intercalating dye from sheath-flow buffer

In order to detect minute amounts (low fg μl^{-1})

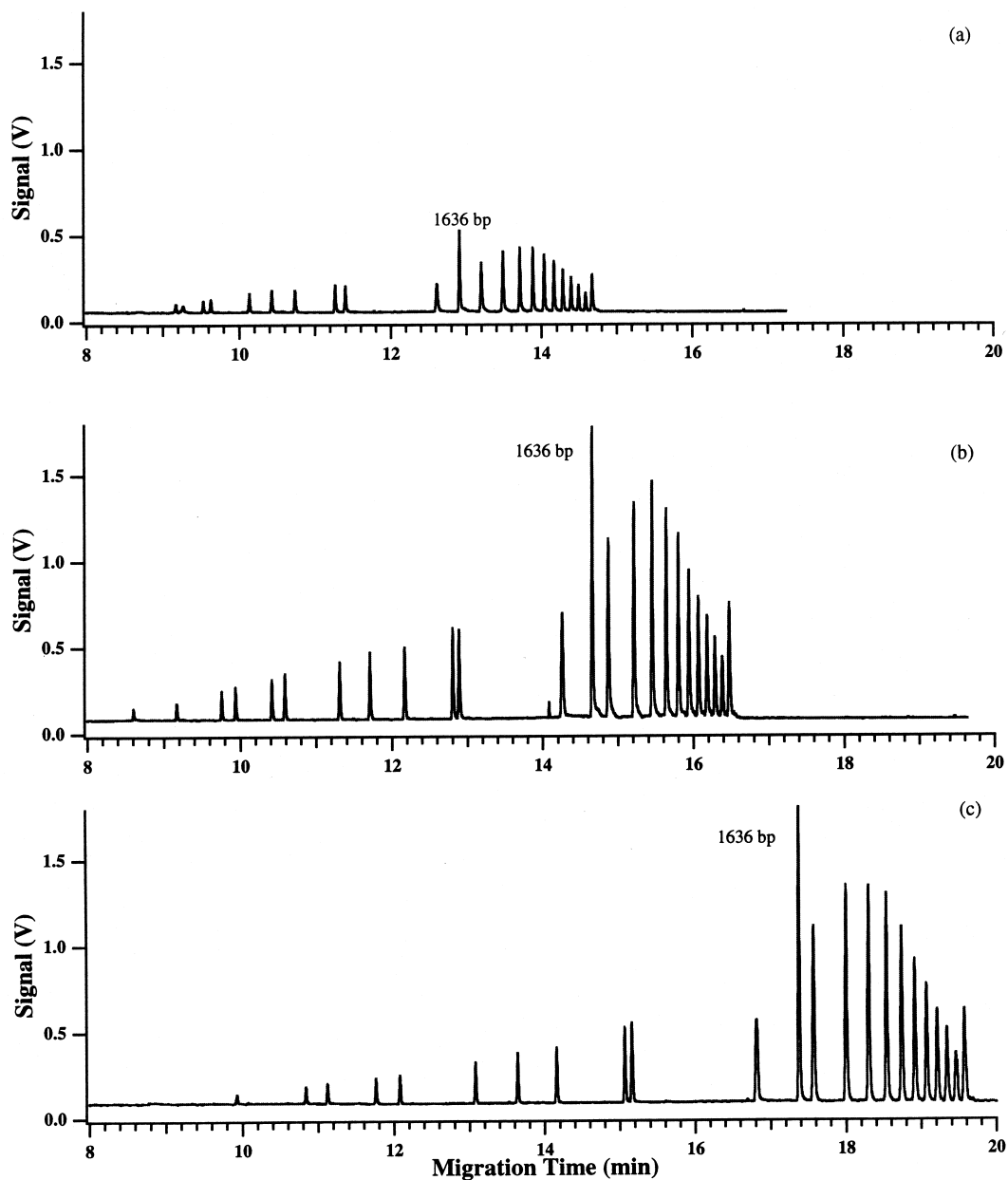


Fig. 4. Comparison of three different dye stacking conditions at the detection end. The separation buffer was 90 mM tris-borate/2 mM EDTA at pH 8.6. (a) sheath buffer was 90 mM Tris-borate/2 mM EDTA at pH 8.6 with $2 \cdot 10^{-7}$ M ethidium bromide homodimer II; (b) sheath buffer was 45 mM Tris base/1 mM EDTA at pH 7 with $2 \cdot 10^{-7}$ M ethidium bromide homodimer II; (c) sheath buffer was 10 mM Tris base/1 mM EDTA at pH 7 with $2 \cdot 10^{-7}$ M ethidium bromide homodimer II.

range) of DNA in the capillary, intercalating dye concentrations between $1 \cdot 10^{-7}$ and $5 \cdot 10^{-7}$ M must be added to the sheath flow buffer to provide optimum labeling without increasing fluorescent background. To achieve low background and a high binding ratio, the dye is prepared in a sheath flow buffer with an ionic strength lower than that of the running buffer, which allows stacking of dye molecules inside the capillary when electric field is applied. This stacked region is sustained by the continuous flow of sheath buffer into the cuvette.

As shown in Fig. 4, stacking of dye molecules enhances the sensitivity of detection by approximately 4-fold (using the 1636 bp fragment as a reference) when there is an approximately 2-fold ionic strength

difference at the boundary of the two buffer systems (Fig. 4b). No substantial increase in sensitivity is observed when the ionic strength difference is increased beyond 2-fold (Fig. 4c). However, a further increase in ionic strength difference improves peak resolution, in particular for the smaller DNA fragments. Separation efficiency remains relatively consistent (6.25% RSD) for all three buffer systems, and there was no observable influence on zone broadening.

3.3. High speed separation

Here, we demonstrate the high speed separation of the 11 fragments from the Φ X174/*HaeIII* digest

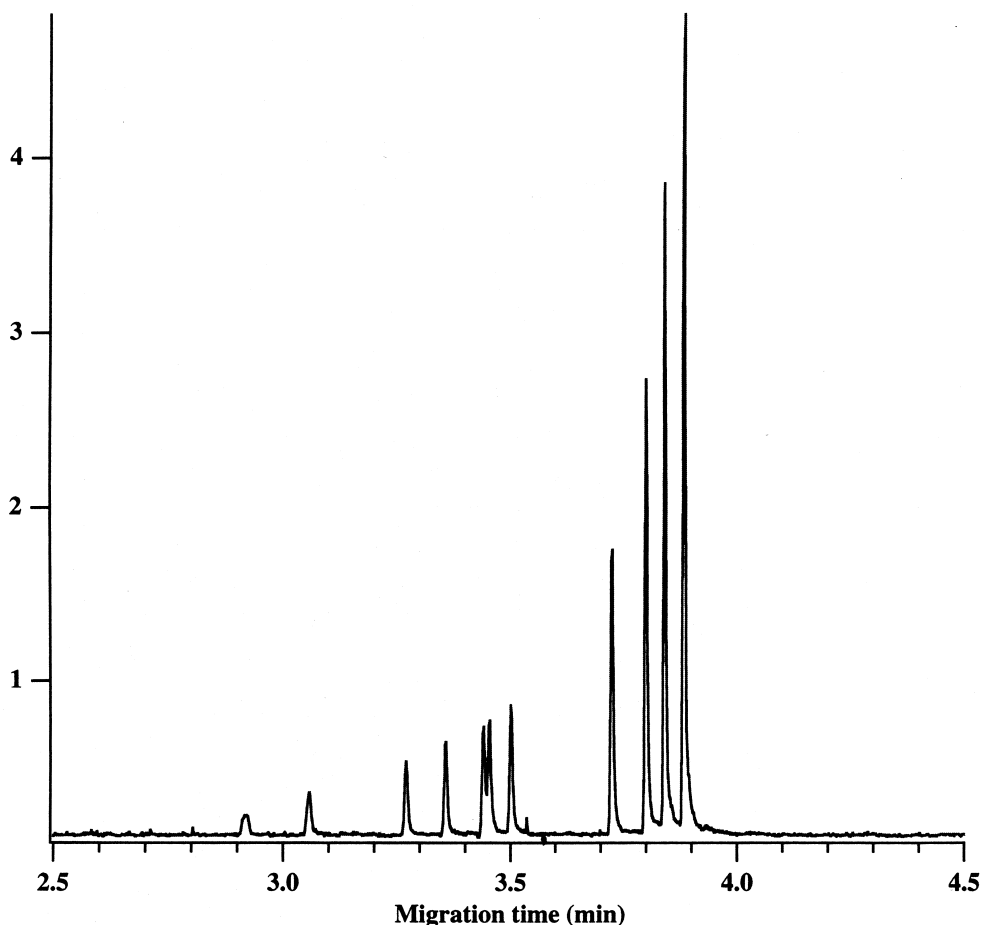


Fig. 5. Separation of restriction DNA fragments at high field strength. Separation of Φ X174/*HaeIII* digest at an electric field of 550 V cm^{-1} . The sheath-flow buffer contained POPO-3.

(Fig. 5). Separation of DNA–dye complexes is achievable at field strength as high as 550 V cm^{-1} as the power generated is usually no higher than 350 mW m^{-1} , a direct result of not adding sodium chloride into the TBE buffer.

3.4. Calibration plots

In Fig. 6 the signal was measured for the $\Phi\text{X174}/\text{HaeIII}$ digest fragments for a total DNA concentration ranging from 5 to $140 \text{ pg } \mu\text{l}^{-1}$. The signal increased linearly with DNA concentration ($r > 0.987$, $n=6$). Sensitivity is proportional to fragment length ($r=0.990$), which results from the constant ratio of dye molecules per base pair. The detection limit (3σ) ranged from $4.7 \cdot 10^{-14} \text{ M}$ for the 1353 bp fragment to $5.3 \cdot 10^{-13} \text{ M}$ for the 72 bp fragment.

To improve detection limit further, a 3021 bp

cloned DHBV genome was used to repeat the same calibration using $2 \cdot 10^{-7} \text{ M}$ ethidium bromide homodimer (EthD2), and increasing the injection time to 20 s at 1 kV. The calibration curve (figure not shown) deviated from linearity for DNA concentration greater than about $5 \text{ pg } \mu\text{l}^{-1}$. In this experiment, the peak width increased dramatically for DNA concentration greater than $4.5 \text{ pg } \mu\text{l}^{-1}$. The detection limit was $3.9 \cdot 10^{-16} \text{ M}$. The long injection period reduced the efficiency to $3\text{--}4 \cdot 10^6$ plates or $\sim 10 \cdot 10^6$ plates m^{-1} .

3.5. Analysis of cloned duck hepatitis B virus DNA fragments

Fig. 7 depicts the separation of cloned duck hepatitis B virus DNA digested with restriction enzyme *HpaII*. All eight fragments generated from the digestion were resolved and clearly separated

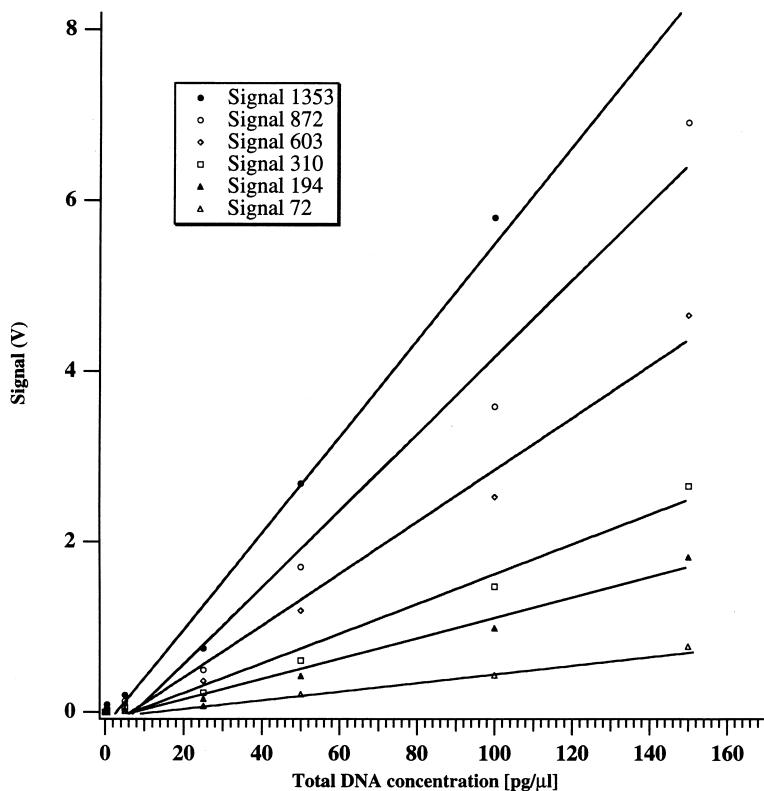


Fig. 6. Calibration plots for $\Phi\text{X174}/\text{HaeIII}$. DNA samples were prepared in deionized water; $1 \times 10^{-7} \text{ M}$ POPO3 was freshly prepared and siphoned into the cuvette. Each sample was injected for 5 s at 1000 V. For clarity, only data set derived from 1353, 872, 603, 310, 194 and 72 bp are shown.

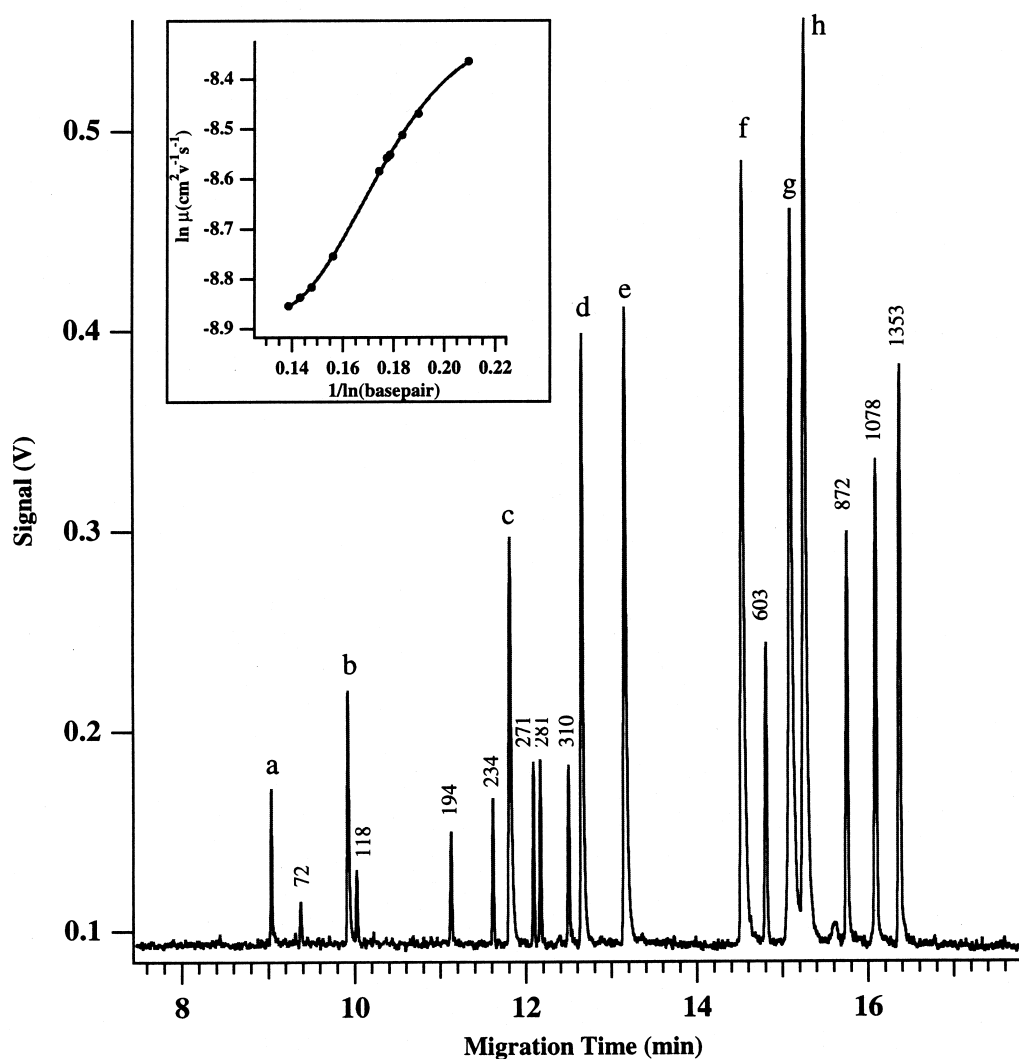


Fig. 7. Separation of duck hepatitis B virus DNA; (a) to (h) represent 8 fragments generated from a *Hpa*II digestion (52, 117, 251, 320, 379, 553, 646 and 703 bp). The sample was spiked with Φ X174/*Hae*III before injection. Final concentration of the molecular mass markers is $60 \text{ pg } \mu\text{l}^{-1}$; concentration of the sample was not determined. Injection was at 1000 V for 5 s; electric field at 200 V cm^{-1} . The calibration ($\ln \mu$ vs. $1/\ln \text{ bp}$) plot in the insert was prepared by least-squares analysis. Stock solution of EthD2 was diluted to $2 \cdot 10^{-7} \text{ M}$ in $45 \text{ mM Tris base}/1 \text{ mM EDTA}$ at pH 7.

from the molecular weight markers containing 11 DNA fragments. The plot of $\ln(\text{mobility})$ vs. $1/\ln(\text{base pair})$ shown in the insert provides a conversion of mobilities of the viral fragments to their corresponding sizes.

Table 1 presents a comparison of the calculated size of the viral DNA fragments, which is in reasonable agreement with that obtained from the literature. DNA size prediction is more accurate

compared to that demonstrated by Rye et al. [28 removed], in which DNA–dye samples were pre-incubated for 30 min at room temperature. According to Carlsson et al. [25], this short incubation time would not be adequate for complete equilibration of DNA–dye complexes. This phenomenon, together with the change of DNA contour length as a result of dye intercalation, may contribute to inaccuracy in predicting DNA size. In our experiments, this dis-

Table 1
Size determination of restriction fragment with ethidium bromide homodimer-2

Peak identity	Actual size ^a (bp)	Calculated size (bp)
a	52	nd
b	117	107
c	251	247
d	320	317
e	379	366
f	553	548
g	646	663
h	703	704

^a Duck hepatitis B virus DNA sequence (HPUCGD accession No. K01834) is obtained from National Center for Biotechnology (<http://www3.ncbi.nlm.nih.gov/BankIt/>); restriction sites for *HpaII* and fragment size were obtained using DNA Strider 1.2 (C. Marck).

crepancy is eliminated because pre-incubation of DNA–dye complexes is not performed prior to sample injection.

Previous studies have shown that single base resolution is usually not possible using a 0.8% HEC polymer solution. However in our studies, the 117 bp viral fragment and the 118 bp size marker were nearly base line resolved. We attribute this unusual resolving power to possible conformational difference between the two unrelated DNA fragments.

4. Concluding remark

As more antiviral options become available and as treatment is commenced at earlier, asymptomatic stages of infection, alternative methods of assessing the efficacy of antiviral regimens are necessary. These methods have to be more sensitive and reliable in order to detect and quantify low viral load in early stages of infection as well as clinical end-point studies such as antiviral therapy for hepatitis B. Using CE–LIF with intercalating dyes, we have improved non-isotopic detectability to the attomole level with sample volumes as small as a few nanoliters.

This allows assessment of disease activity in chronic infection. Low HBV DNA values (<100 pg ml⁻¹) imply low HBV replication, and high HBV DNA values (>100 pg ml⁻¹) indicate a higher

degree of viral replication, allowing differential treatment regimens to be selected [1]. However, in patients undergoing antiviral therapy where viral load can be as low as less than 1 pg ml⁻¹, the CE–LIF method will require a sample pre-concentration step in order to evaluate viral loading.

Acknowledgements

This work was supported by the Canadian Bacterial Diseases Network and by the Natural Sciences and Engineering Research Council. The authors thank Dr. E. Arriaga for technical assistance on the instrument set up, Dr. C. Stathakis for his valuable input and critical review of the paper before submission, and all NLLL members for support of this study. Plasmid pAltD2–8 was a generous gift from Dr. K. Fisher (Glaxo Heritage Research Institute).

References

- [1] S. Aspinall, A.D. Steele, I. Peenze, M.J. Mphahlele, J. Viral Hepatitis 2 (1995) 107.
- [2] K.C. Chan, C.W. Whang, E.S. Yeung, J. Liquid Chromatogr. 16 (1993) 1941.
- [3] D.A. McGregor, E.S. Yeung, J. Chromatogr. A 652 (1993) 67.
- [4] M.H. Kleemiß, M. Gilges, G. Schomburg, Electrophoresis 14 (1993) 515.
- [5] P.E. Williams, M.A. Marino, S.A. Del Rio, L.A. Turni, J.M. Devaney, J. Chromatogr. A 680 (1994) 525.
- [6] D.A. McGregor, E.S. Yeung, J. Chromatogr. A 680 (1994) 491.
- [7] W. Lu, D.S. Han, J. Yuan, J.M. Andrieu, Nature 368 (1994) 269.
- [8] Y. Baba, N. Ishimaru, K. Samata, M. Tsuhako, J. Chromatogr. A 653 (1993) 329.
- [9] A.W.H.M. Kuypers, P.M.W. Willems, M.J. van der Schans, P.C.M. Linssen, H.M.C. Wessels, C.H.M.M. de Bruijn, F.M. Everaerts, E.J.B.M. Mensink, J. Chromatogr. 621 (1993) 149.
- [10] K.R. Mitchelson, J. Cheng, J. Cap. Electrophoresis 2 (1995) 137.
- [11] J. Cadet, M. Weinfeld, Anal. Chem. 65 (1993) 675A.
- [12] J.P. Landers, R.P. Oda, T.C. Spelsberg, J.A. Nolan, K.J. Ulfelder, Bio Techniques 14 (1993) 98.
- [13] H.E. Schwartz, K.J. Ulfelder, Anal. Chem. 64 (1992) 1737.
- [14] D. Figeys, E. Arriaga, E. Renborg, N.J. Dovichi, J. Chromatogr. A 669 (1994) 205.

- [15] K. Srinivasan, J.E. Girard, P. Williams, R.K. Roby, V.W. Weedn, S.C. Morris, M.C. Kline, D.J. Reeder, *J. Chromatogr. A* 652 (1993) 83.
- [16] H. Zhu, S.M. Clark, S.C. Benson, H.S. Rye, A.N. Glazer, R.A. Mathies, *Anal. Chem.* 66 (1994) 1941.
- [17] R.P. Haugland, *Molecular Probes*, Eugene, OR, 1992, p. 221.
- [18] J. Berka, Y.F. Pariat, O. Muller, K. Hebenbrock, D.N. Heiger, F. Foret, L.B. Karger, *Electrophoresis* 16 (1995) 377.
- [19] Y. Kim, M.D. Morris, *Anal. Chem.* 66 (1994) 1168.
- [20] D.M. Crothers, *Biopolymers* 6 (1968) 575.
- [21] R.G.M. Wright, L.P.G. Wakelin, A. Fieldes, R.M. Acheson, M.J. Waring, *Biochemistry* 19 (1980) 5825.
- [22] N. Assa-Munt, W.A. Denny, W. Leupin, D.R. Kearns, *Biochemistry* 24 (1985) 1441.
- [23] J. Markovits, B.P. Roques, J.B. Le Pecq, *Anal. Chem.* 94 (1979) 259.
- [24] J. Skeidsvoll, P.M. Ueland, *Anal. Biochem.* 231 (1995) 359.
- [25] C. Carlsson, M. Jonsson, B. Akerman, *Nucleic Acids Res.* 23 (1995) 2413.
- [26] K. Srinivasan, S.C. Morris, J.E. Girard, M.C. Kline, D.J. Reeder, *Appl. Theor. Electrophoresis* 3 (1993) 235.
- [27] B.K. Clark, M.J. Sepaniak, *J. Microcol. Sep.* 5 (1993) 275.
- [28] H.P. Swerdlow, S. Wu, H.R. Harke, N.J. Dovichi, *J. Chromatogr.* 516 (1990) 61.